North Carolina Agricultural and Technical State University

Aggie Digital Collections and Scholarship

2010

Study Of Nanodiamonds Using Molecular Dynamic Simulations With Reactive Potentials

Ferdaus Faruq
North Carolina Agricultural and Technical State University

Follow this and additional works at: https://digital.library.ncat.edu/theses

STUDY OF NANODIAMONDS USING MOLECULAR DYNAMIC SIMULATIONS
WITH REACTIVE POTENTIALS

by

Ferdaus Faruq

A thesis submitted to the graduate faculty
in partial fulfillment of the requirements for the degree of
MASTER OF SCIENCE

Department: Chemical and Bioengineering
Major: Chemical Engineering
Major Professor: Dr. Vinayak Kabadi

North Carolina A&T State University
Greensboro, North Carolina
2010

School of Graduate Studies
North Carolina Agricultural and Technical State University

This is to certify that the Master's Thesis of

Ferdaus Faruq

has met the thesis requirements of
North Carolina Agricultural and Technical State University

Greensboro, North Carolina
2010

Approved by:

_____ _____
Dr. Vinayak Kabadi   Dr. Shamsuddin Ilias
Major Professor   Committee Member

_____ _____
Dr. John Kizito   Dr. Leonard C Uitenham
Committee Member   Department Chairperson

_____
Dr. Alan Letton
Interim Associate Vice Chancellor of
Research and Graduate Dean

DEDICATION

I dedicate this to my wife, for her love and support.

BIOGRAPHICAL SKETCH

Ferdaus Faruq was born on January 30th, 1985 in New York City, New York. He received the Bachelor of Arts degree in Physics in 2008 from Grinnell College. He joined the Master of Science program in Chemical Engineering in the Fall of 2008 as a Research Assistant at North Carolina Agricultural and Technical State University. He is a candidate for the Masters of Science in Chemical Engineering.

ACKNOWLEDGMENTS

I would like to express gratitude and appreciation to my advisor, Dr. Vinayak Kabadi, for his encouragement, supervision, and advice throughout this research. His moral support and continuous suggestions enabled me to complete my work successfully. I am also thankful to me committee members for their valuable recommendations.

I would also like to acknowledge the Department of Chemical Engineering at North Carolina A&T State University for providing the financial assistance for this research. I would like to thank Dr. Shamsuddin Ilias for making all of this possible.

TABLE OF CONTENTS

LIST OF FIGURES

LIST OF TABLES

LIST OF SYMBOLS

ω^s Angular velocity, frame of reference pertaining to the simulation box

θ Euler angle, rotation about x axis

ψ Euler angle, rotation about y axis

φ Euler angle, rotation about z axis

$R(n)$ Bond length as function of bond order n

r_{ij} Distance between atoms i and j

b_{ij} Bond order between atoms i and j

θ_{ijk} Angle between atoms i,j, and k

V_A Attractive potential

V_R Repulsive potential

ω_{ijkl} Dihedral angle between atoms i,j,k and l

ABSTRACT

Faruq, Ferdaus. STUDY OF NANODIAMONDS USING MOLECULAR DYNAMIC SIMULATIONS WITH REACTIVE POTENTIALS. (**Major Advisor: Vinayak Kabadi**), North Carolina Agricultural and Technical State University.

This thesis pertains to the application of classical molecular dynamic simulations using reactive potentials to create a stable nanodiamond with properties as determined by quantum simulations. Nanodiamonds possess large amounts of Structural Bond Energy (SBE) and they have internal pressures as high as 50 GPa. Nanodiamonds could be used as potential energetic materials if their bond energy could be released. The simulations described here incorporated reactive potentials such as AIREBO (Adaptive Intermolecular Reactive Empirical Bond Order) and ReaxFF (Reactive Force Field), since they are able to describe the breaking and forming of bonds. The simulation package LAMMPS (Large-scale Atomic/Molecular Massively Parallel Simulator) was used.

A fullerene shell was placed over the bulk diamond structure to create the nanodiamond. NPT and NVE simulations were performed. The main objective of this thesis is to describe a systematic approach of generating thermodynamically stable nanodiamonds using molecular dynamic simulations. For further research, the stable nanodiamonds will be used to simulate high velocity collisions between multiple nanodiamonds to determine the rate and release of SBE.

CHAPTER 1

INTRODUCTION

Nanodiamonds are comprised of nanometer sized diamond cores incased in fullerene shells. These molecules have been discovered in carbonaceous residues of detonations as well as in interstellar dust and in meteorites [1]. Although nanodiamonds are formed under extreme conditions, once formed they are able to maintain their structures under normal atmospheric conditions.

Nanodiamonds are of significant research interest due to their unique structure. The fullerene shell, which encases the diamond core, applies significant pressure to the core reported to be around 50 GPa by Mattson [2]. This high pressure significantly increases the bond energies in the diamond core. These bond energies are known as Structural Bond Energy (SBE). Researchers have found that rupturing the fullerene shell will facilitate the release of SBE in the diamond core, which could potentially cause other nanodiamonds to rupture in a manner similar to chain reactions. This is why release of SBE (SBER) is of significant interest. Measuring the rate of SBER could determine whether or not nanodiamonds are potential energetic materials. However, all research done on the bond energy of the nanodiamond has been limited to quantum mechanical simulations [2][3]. Although these simulations provide a more accurate description of the bond energies, they are limited by computing power. For example, Mattson was able to simulate the collision between two nanodiamonds and observe that smaller carbon chains

produced from the resulting collision were energetic enough to break apart other nanodiamonds. However, Mattson's work would have to be repeated with more nanodiamonds in order to confirm these results.

The purpose of this research is to apply classical molecular dynamic simulations using reactive potentials to create a stable nanodiamond. The main objective of this research is to establish a systematic method of generating thermodynamically stable nanodiamonds using these simulations. Molecular dynamic simulations will be used since they are significantly less computation intensive than quantum simulations. The molecular dynamic simulations can be used to test whether a diamond structure evolves into a nanodiamond, as has been reported by researchers using quantum simulations. The simulations performed in this research will incorporate reactive potentials such as AIREBO and ReaxFF, since they are able to describe the breaking and forming of bonds, although not as accurately as quantum simulations.

CHAPTER 2

BACKGROUND

2.1 Nanodiamonds

There is significant research regarding the formation of nanodiamonds. Researchers such as Titov et al [3], have found that nanodiamonds can be formed in laboratory experiments using the detonation of a TNT/RDX mixture. Using a method of X-ray scattering, they were able to measure the amount of nanodiamonds formed and the time at which they are formed. It was found that placing a shell over the detonation alters the rarefaction of the detonation shock wave, which in turn affects the kinetics of the nanodiamond growth. Titov et al observed that the rate at which the nanodiamonds are formed is reduced as the thickness of the shell is increased.

The chemical properties of nanodiamonds have also been widely researched. Researchers such as Brodka et al [4], have found that with adequate heating, nanodiamonds can be graphitized. Using molecular dynamic simulations, they were able to create carbon onions from the nanodiamonds. The graphitization process involves the breakage of certain bonds in the nanodiamond structure, which creates a structure similar to graphite. However in this case, the graphite layers are spherical, resembling an onion. Brodka et al found that this process begins at around 1200 K while full graphitization occurs at around 1500 K. Other studies have considered the affects of impurities in the nanodiamond. Barnard et al [5] introduced nitrogen into the structure of the nanodiamond

using quantum simulations. They found that the nitrogen substitution occurs primarily in the fullerene shell of the nanodiamond, and produces a slightly negative net charge in the carbon atoms. Hence understanding the effects of doping or temperature on the chemical properties of the nanodiamond is necessary for practical applications, such as nanodevices, where nanodiamonds would be used as semiconductor-like material.

The key aspect of this research is the unique structural property of the nanodiamonds, that is, the fullerene shell surrounding the compressed diamond core. The substantial increase in SBE due to the compression of the diamond core translates into a larger amount of kinetic energy released once the bonds are broken. This increased kinetic energy, has implications for energy production and explosives. In fact rapid release of SBE has been shown to create explosions. There has been some research done regarding the release of the bond energies, however these involve quantum simulations. Mattson et al [2] observed from the simulated collision of the two nanodiamonds that large amounts of mono- and multi-atomic fragments are produced at high velocities, which might be highly reactive. The actual reactivity of this process is unknown since systems larger than two nanodiamonds would be necessary to obtain reasonable results. To study the rate of SBER, as done by Mattson et al, a large stable system of nanodiamonds will be needed to simulate high velocity collisions. Therefore, the nanodiamonds used for the collision simulations need to comply with the properties observed by Mattson et al when they relaxed the bulk diamond structure to produce a nanodiamond.

2.2 Computer Simulations

Scientific studies for the most part have been done in laboratories involving physical measurements and observations. In recent times due to the massive hardware improvements and miniaturization of computers, it is feasible to perform simulations of systems based on theoretically derived mathematical models. The results of these can then be used to test theoretical predictions and to provide comparison for experimental data. Computer simulations can be invaluable tools for researchers provided that they are used in the proper manner.

Molecular simulations are used to create a virtual, near accurate representation of particle interactions at the molecular level. In a laboratory setting, it is usually difficult, and in many cases impossible, to study certain molecular systems and their behaviors especially in the nanometer scale. Systems which require extreme temperatures and pressures, such as shock waves, high temperature plasma, etc. would be difficult to deal with under laboratory settings. However, provided the right model is used, a simulation would be highly effective in providing observable results in these cases. One area where simulations have a great advantage is the observation of events which occur in infinitesimal fractions of time, for example in chemical reactions. Events observed in a simulation in the microscopic scale can be used to study macroscopic properties (equation of state, transport coefficients, etc) [6].

There are two main disadvantages regarding the use of simulations. The first is the fact that mathematical models are used to quantify real world interactions. Regardless of how well developed a model is, it cannot be perfectly realistic and can therefore not

cover all possible scenarios and/or outcomes. It is therefore extremely important that the correct model is used for a given system, so as to represent the system as accurately as possible. The second problem is hardware limitations. Computing power has increased exponentially over the years, which should mitigate the demands of simulations. But the increase in computing power has allowed researchers to take on more complex systems, which in turn are stretching the limits of currently available computing power and eventually better hardware will be necessary to facilitate even more computation intensive problems.

Molecular dynamic (MD) simulations are performed by solving Newton's equations of motion for each particle within a system. Essentially, this means solving a set of three differential equations for each molecule in order to determine the position and velocity at each time step. This research will use the same method to simulate an equilibrium system of nanodiamonds. Another form of MD simulation, called non-equilibrium MD simulations, is used for systems with thermodynamic fluxes [6]. This is useful for modeling systems with heat flow, shearing, etc.

2.3 Molecular Dynamic Simulation Process

Molecular Dynamic simulations have been used since the late 1950s. Initially, they were used to simulate hard-sphere particles traveling at constant velocities which were collided elastically. Later the Lennard-Jones potential was applied, which brought forth rapid developments in the MD simulation process.

The MD simulation can be split into three areas of focus: 1) initial positions and orientations, 2) interactive potentials, and 3) time integration. The initial positions are necessary for solving the equations of motion while the orientation of the molecules directly influences the manner in which the potential energy function behaves since it takes into account bond angles and dihedrals, which affect the rotational energy of each molecule. The interactive potential takes into account the intermolecular and interatomic interactions within the system, from which the forces exerted on all species can be calculated. Time integration updates the positions and velocities of each atom at every time step based on the behavior modeled by the interactive potential and the initial positions and orientations of the species in the system. The following sections provide a discussion on the core elements of a properly functioning MD simulation.

This research incorporates two types of simulations which are NVE and NPT simulations. 'NVE' signifies a system where the number of atoms, the system volume and the total energy are kept constant. The total energy (the sum of potential and kinetic energy) is kept constant by the concept of conservation of energy, that is potential energy is converted to kinetic energy when bonds are broken and vice versa. The equations of motion are solved (based on the potential and kinetic energy) and the positions and velocities are updated every subsequent time step.

NPT simulations impose an isobaric and isothermal condition to the system. LAMMPS achieves this by applying a Nose-Hoover thermostat and a Nose-Hoover barostat as implemented by Melchionna et al [7]. According to Melchionna et al, the Nose-Hoover thermostat provides equations of motions that are easily solvable when

volume is kept constant. However, in the case of the barostat, volume cannot be constant. Due to this, solving the equations of motion based on the Nose-Hoover algorithm would be difficult. In order to obtain a set of solvable equations of motion using the Nose-Hoover algorithm, Melchionna et al modified said algorithm, to introduce a piston strain factor term to the velocity expression in order to stabilize the deviations due to the difference between the instantaneous pressure and desired pressure. This allows for the equations of motion to be obtained without increasing the degrees of freedom.

2.3.1 Position and Orientation

The positions of the atoms in a system are usually defined by a series of vectors containing the x, y, and z coordinates (depending on whether the system is 2 or 3 dimensional). In the case of LAMMPS, the initial positions of the atoms can be generated by using a built in function, such as *fcc* which generates the positions based on the face centered cubic lattice formation, or can be user defined, which involves a data file containing the position vector of each atom in the system. When setting the initial positions (whether by using a built in function or user specified coordinates), it must be taken into account that they correspond to the desired density, otherwise the simulation will be erroneous.

For simulations involving monoatomic systems, orientation does not serve much of a purpose, however when simulating many-body systems, keeping track of the orientation is necessary. As the system evolves due to time integration, forces exerted on certain molecules may induce a rotational velocity will change their orientation over time. In order to keep track of this, Euler angles are used. These angles are able to keep

track of rotation about the center of mass based on the desired frame of reference which can be the simulation box or with respect to another atom or molecule. These are used specifically for systems containing rigid molecules.

The Euler angles are θ, ψ, and φ, which are rotation about the x axis, rotation about the y axis, and rotation about the z axis respectively. The rotation is defined by the matrix expression [8]:

$$\mathbf{x}' = A\mathbf{x} \tag{2.1}$$

where,

$$A = \begin{bmatrix} \cos\phi\cos\psi - \cos\theta\sin\psi\sin\phi & \cos\psi\sin\phi + \cos\theta\sin\psi\cos\phi & \sin\theta\sin\psi \\ -\sin\psi\cos\phi - \cos\theta\cos\psi\sin\phi & -\sin\psi\sin\phi + \cos\theta\cos\psi\cos\phi & \sin\theta\cos\psi \\ \sin\theta\sin\phi & -\sin\theta\sin\phi & \cos\theta \end{bmatrix} \tag{2.2}$$

In Equation 2.1, $\mathbf{x}'$ refers to the updated positions of the atoms after rotation has been taken into account. Using these expressions, a system of equations of motion is formed with respect to angular velocity:

$$\begin{aligned} \dot{\phi} &= -\omega_x^s \frac{\sin\phi\cos\theta}{\sin\theta} + \omega_y^s \frac{\cos\phi\cos\theta}{\sin\theta} + \omega_z^s \\ \dot{\theta} &= \omega_x^s \frac{\sin\phi}{\sin\theta} - \omega_y^s \frac{\cos\phi}{\sin\theta} \\ \dot{\psi} &= \omega_x^s \frac{\sin\phi}{\sin\theta} - \omega_y^s \frac{\cos\phi}{\sin\theta} \end{aligned} \tag{2.3}$$

where, ω^s is the angular velocity vector based on the frame of reference of the simulation box. It is clear from Equation 2.3 that there will be problems when θ approaches 0° and 180°. In order to circumvent these singularities, Evans [9] used four quaternion parameters used in the form:

$$q_0^2 + q_1^2 + q_2^2 + q_3^2 = 1 \tag{2.4}$$

where,

$$
\begin{aligned}
q_0 &= \cos\frac{\theta}{2}\cos\frac{\phi+\psi}{2} \\
q_1 &= \sin\frac{\theta}{2}\cos\frac{\phi-\psi}{2} \\
q_2 &= \sin\frac{\theta}{2}\sin\frac{\phi-\psi}{2} \\
q_3 &= \cos\frac{\theta}{2}\sin\frac{\phi+\psi}{2}
\end{aligned} \tag{2.5}
$$

The resulting rotation matrix becomes:

$$
A = \begin{bmatrix}
q_0^2 + q_1^2 - q_2^2 - q_3^2 & 2(q_1q_2 + q_0q_3) & 2(q_1q_3 - q_0q_2) \\
2(q_1q_2 - q_0q_3) & q_0^2 - q_1^2 + q_2^2 - q_3^2 & 2(q_3q_2 + q_0q_1) \\
2(q_1q_3 + q_0q_2) & 2(q_3q_2 - q_0q_1) & q_0^2 - q_1^2 - q_2^2 + q_3^2
\end{bmatrix} \tag{2.6}
$$

10

From Equations 2.4 and 2.6 it can be seen that, with Euler angles, quaternions are able to keep track of orientation in a straight forward manner.

2.3.2 Interactive Potentials

When considering the simulation of a molecular system, one needs to take into account the interaction between molecules in order to successfully determine the positions and velocities of the particles at the end of a time step. In order to achieve this, an empirical formula is used to mathematically describe these intermolecular interactions.

According to Tildesley [6], the total energy of the system is summed up as the Hamiltonian (which is an equation of motion). The Hamiltonian can be described as the sum of the functions of kinetic energy and potential energy. For the molecules, the kinetic energy is a function of momentum while the potential energy is a function of position. The potential energy function (or force fields) is of interest since it describes the intermolecular interactions. Various forms and descriptions of these potentials which are of relevance to this research are given in the following sections.

Based on their relevance in this research, two particular force fields and their development will be discussed. These potentials are AIREBO and ReaxFF. These represent styles with which chemical reactions between specific species can be simulated. Although they are represented by dissimilar empirical expressions, they both are given in terms of bond orders.

Bond orders represent the type of bond found between different species. For example, the bond order for nitrogen in a nitrogen molecule (N_2) is two since there is a double bond between the two atoms. For a classical simulation to be carried out for a

chemical reaction it is necessary to determine the bond type from the local geometry of the atoms and molecules present in the chemical reaction simulation.

Using the Pauling relationship [10] between bond length and bond order, it is possible to determine types of bonds in a classical simulations (both AIREBO and ReaxFF incorporates Pauling's relationship). This relationship is described as:

$$R(1) - R(n) = 0.300 \log n \tag{2.7}$$

Here, *R(1)* represents the length of a single bond and is used as a reference, while *R(n)* represents the length of the bond of order *n*. The constant 0.300 has been used by Pauling since that value agrees well with the covalent bond distances found experimentally [9]. Hence using the reference *R(1)*, it would be possible to determine the length of *R(2)* and *R(3)*. For example, *C-C* bond distances are found to be 1.542, 1.330 and 1.204 Å for a single, double and triple bond respectively. In a simulation, if an atom is found to be further than 1.542 Å from another atom, the bond order between the two is taken to be 0; however if the atom is found to be around 1.3 Å, a bond order of 2 will be considered. This example is quite simplistic since other factors such as repulsion and bond angles are taken into account to actually determine the presence of a bond.

As mentioned before, the AIREBO potential is a bond order potential. AIREBO which stands for Adaptive Intermolecular REBO potential, is a modified form of the REBO potential (Reactive Empirical Bond Order potential) developed by Brenner [11].

The REBO potential is in turn a modified version of the Tersoff potential, which again was based on the Morse potential.

2.3.2.1 Morse Potential

The Morse potential was developed by Philip M. Morse in 1929. The potential was derived from the exact solution of Schroedinger's equation for nuclei in a diatomic molecule [12]. By starting with the equation:

$$\nabla^2 \psi + \frac{8\pi^2 \mu}{h^2}\left[W - \left(\frac{e^2 Z_1 Z_2}{r}\right) + V_e(r)\right]\psi = 0 \tag{2.8}$$

where, ψ is the wave function, μ is given as $\dfrac{1}{M_1} + \dfrac{1}{M_2}$ where M_1 and M_2 are the atomic masses of the diatomic molecule, r is the distance between the nuclei and $V_e(r)$ is the electronic energy calculated by fixing the two nuclei by a distance of r. In the above expression, $\left(\dfrac{e^2 Z_1 Z_2}{r}\right) + V_e(r)$ represents the repulsive energy and the electronic energy which is taken to be $E(r)$. By replacing Ψ with $N\Phi(\varphi)\Theta(\theta)R(r)/r$, where N is the normalizing factor and Φ and Θ represent the orientation angles based on the center of gravity and R is a wave function, the previous equation becomes:

$$\frac{d^2 R}{dr^2} + \frac{j(j+1)R}{r^2} + \frac{8\pi^2 \mu}{h^2}[W - E(r)]R = 0 \tag{2.9}$$

where j is the vibration level. By taking the function $E(r) = De^{-2a(r-r_0)} - 2De^{-a(r-r_0)}$, an exact solution of Schroedinger's equation was obtained and the values for D and a were found to be $\omega_0^2/4\omega_0 x$ and $0.2454(M\omega_0 x)^{\frac{1}{2}}$ respectively where ω_0 and $\omega_0 x$ are constants in wave-numbers. This potential does not take into account reactivity and is ideal for diatomic systems. However, the potential energy functions derived by Morse lays the groundwork for further improved potentials, some of which facilitates the breaking and formation of bonds.

2.3.2.2 Tersoff Potential

Using the results for the potential calculated by Morse, Tersoff [13] obtained an expression for a potential (known as Tersoff potential) based on the idea of bond orders. It arises from the fact that the more neighbors an atom has the weaker the bond between the atom and its neighbors will be. As a result the bond strength or bond order depends on the geometry of the molecules in the system.

The Tersoff potential is described by the following expression:

$$E = \frac{1}{2}\sum_{i \neq j} V_{ij} \tag{2.10}$$

$$V_{ij} = f_c(r_{ij})[a_{ij}f_R(r_{ij}) + b_{ij}f_A(r_{ij})] \tag{2.11}$$

where E is the total energy of the system, V_{ij} is the bond energy, and r_{ij} is the distance between atom i and atom j, f_R and f_A are the repulsive and attractive pair potentials

14

respectively and are defined by Morse-like potentials, that is $f_R(r) = Ae^{-\lambda_1 r}$ and $f_A(r) = -Be^{-\lambda_2 r}$. The parameters A, B, λ_1, and λ_2 vary depending on the type of atom.

The term b_{ij} represents the bond order term. This term essentially gives weight to the attractive potential in the above expression, that is, the greater the bond order the greater the overall attractive potential. The term b_{ij} is represented by the following equations:

$$b_{ij} = (1 + \beta^n \zeta_{ij}^n)^{-\frac{1}{2n}} \tag{2.12}$$

$$\zeta_{ij} = \sum_{k \neq i,j} f_c(r_{ij}) g(\theta_{ijk}) e^{[\lambda_3^3 (r_{ij} - r_{ik})^3]} \tag{2.13}$$

$$g(\theta) = 1 + \frac{c^2}{d^2} - \frac{c^2}{[d^2 + (h - \cos\theta)^2]} \tag{2.14}$$

where θ_{ijk} represent the bond angle between atoms i, j and i, k. The expression for b_{ij} indicates that it is solely a function of bond length and bond angle. Hence the bond order takes into account the local geometry of the system.

The parameter a_{ij} is given by the following forms:

$$a_{ij} = (1 + \alpha^n \eta_{ij}^n)^{-\frac{1}{2n}} \tag{2.15}$$

$$\eta_{ij} = \sum_{k \neq i,j} f_c(r_{ij}) e^{[\lambda_3^3 (r_{ij} - r_{ik})^3]} \tag{2.16}$$

The expression for a_{ij} is functionally similar to the expression b_{ij} however a_{ij} is not dependant on θ. α is taken in such a way that it is very small, thus making $a_{ij} \cong 1$.

All the expressions given above contain a parameter f_c which is known as the cut-off function and is used to produce a continuous value for all derivatives of r. It also ensures that the potential behaves as a short range potential, only calculating values for energies of particles around the first-neighbor cell.

f_c is given by:

$$f_c(r) = \begin{cases} 1, r < R - D \\ \dfrac{1}{2} - \dfrac{1}{2}\sin\left[\dfrac{\pi(r-R)}{2D}\right], R - D < r < R + D \\ 0, r > R + D \end{cases} \tag{2.17}$$

where, R and D represent the shell where values f_c can be calculated. When an atom j is at a distance greater than the shell of atom i (i.e. $R+D$), the value for f_c is zero, which implies that the bond energy between i and j is zero.

Apart from applying attractive and repulsive pair potentials as derived by Morse [12], the Tersoff potential incorporates the bond order. This allows for the potential to describe more complex covalent systems, such as in silicon and carbon. However, this is strictly a short range potential and lacks the terms to describe long range and non-bonded interactions. Although the Tersoff potential takes into account the bond order and the formation and breaking of bonds, it is applicable to systems with only a single species, which reduces the effectiveness of this potential. The bond order is present to correct the

16

energy of the system based on the strength of the bonds. Advanced potentials like REBO and AIREBO incorporates a variation of Equation 2.10 to describe bond energies.

2.3.2.3 REBO Potential

The Reactive Empirical Bond Order potential or REBO potential is a Tersoff-like potential developed by Brenner [11]. Like the Tersoff potential, the REBO potential successfully simulates short range covalent bonding. However the main difference between the two potentials is that REBO can calculate bond energies for atoms of different coordinations. For example, while the Tersoff potential can describe the covalent bonding in a system of carbon atoms only, the REBO potential can handle a hydrocarbon system. This makes REBO very useful in describing a system of multiple species.

In the same style as the Tersoff potential, the REBO potential is defined as:

$$E_b = \sum_i \sum_{j(>i)} [V_R(r_{ij}) - \bar{B}_{ij} V_A(r_{ij})] \tag{2.18}$$

where V_R, V_A, and $\bar{B}_{ij}$ represent the repulsive potential, attractive potential and bond order respectively. $\bar{B}_{ij}$ is the average of B_{ij} and B_{ji} in addition to a correction factor F_{ij} which corrects for instances of over coordination and is a function of the total number of neighboring atoms and the number of conjugate bonds between them. Note that $B_{ij} \neq B_{ji}$ since atoms of different bond orders are present. The bond order expression here has been modified from the bond order given in the Tersoff potential. The bond order is defined as:

$$B_{ij} = \left[1 + \sum_{k(\neq i,j)} G_i(\theta_{ijk}) f_{ik}(r_{ik}) e^{\alpha_{ijk}[(r_{ij}-R_{ij}^{(e)})-(r_{ik}-R_{ik}^{(e)})]} + H_{ij}(N_i^{(H)}, N_i^{(C)}) \right]^{-\delta} \qquad (2.19)$$

where $R_{ij}^{(e)}$ is the equilibrium distance and the additional term $H_{ij}(N_i^{(H)}, N_i^{(C)})$ incorporates the number of hydrogen and carbon atoms bonded to atom i.

The terms V_R and V_A are taken to be slightly modified forms of the Morse potential, and are given below:

$$V_R(r_{ij}) = \frac{f_{ij}(r_{ij}) D_{ij}^{(e)} e^{-\sqrt{2S_{ij}}\beta_{ij}(r-R_{ij}^{(e)})}}{(S_{ij}-1)} \qquad (2.20)$$

$$V_A(r_{ij}) = \frac{f_{ij}(r_{ij}) D_{ij}^{(e)} S_{ij} e^{-\sqrt{\frac{2}{S_{ij}}}\beta_{ij}(r-R_{ij}^{(e)})}}{(S_{ij}-1)} \qquad (2.21)$$

As can be seen, the expressions above are essentially equivalent to the Morse potential expressions given previously. In fact if S_{ij} is taken to be 2, both terms reduce down to exactly the Morse potentials. The values for $D_{ij}^{(e)}$, $R_{ij}^{(e)}$, and β_{ij} are equal to the equivalent parameter values given in the paper by Morse [12]. The function f_{ij} (which is equivalent to the cutoff function) and $G_i(\theta)$ are the same as the f_c and g functions found in the Tersoff potential.

Although this potential can simulate hydrocarbons it has its shortcomings. The potential makes fitting equilibrium distances and energies restrictive. Also, it provides

only finite values as the distance between molecules decrease [14]. In order to improve on these short comings, the original REBO potential was updated by Brenner in 2001. The second generation REBO potential still retained its basic form, that is:

$$E_b = \sum_i \sum_{j(>i)} [V_R(r_{ij}) - \bar{B}_{ij} V_A(r_{ij})] \qquad (2.22)$$

However, V_R and V_A were modified as follows:

$$V_R(r) = f_c(r)\left(1 + \frac{Q}{r}\right) A e^{-\alpha r} \qquad (2.23)$$

$$V_A(r) = f_c(r) \sum_{n=1,3} B_n e^{-\beta_n r} \qquad (2.24)$$

From the expression of V_R it can be seen that as r gets closer to zero the function tends to infinity. Also due to the reduced number of parameters fitting the potential is simpler. Although the REBO potential can be used to simulate hydrocarbon and diamond systems, it is still a short range potential, hence lacking the ability to describe non-bonded interactions. The REBO potential is more useful than the Tersoff potential since it can simulate systems with multiple species. However, both potentials are short ranged and are not useful for complex systems.

2.3.2.4 AIREBO potential

The AIREBO potential [15] is a modified form of the REBO potential. The manner in which the REBO potential was formulated took into account only the

intermolecular interactions between a molecule and its closest neighbors. However, it is not able to model the interactions in a system with a significant amount of non bonded molecules. Also, it does not take into account the torsional effects observed in long chained hydrocarbons. For these reasons, the REBO potential is not suitable for simulating the systems that contain significant amounts of non bonded long chain hydrocarbons. In order to improve upon these deficiencies, Stuart et al [15] developed a potential which incorporated the non bonded and torsional potentials. The expression is as follows:

$$E = E^{REBO} + E^{LJ} + E^{tors} \tag{2.25}$$

In the above expression, E^{REBO} is identical to that of the second generation REBO potential discussed earlier and no changes were made to it. E^{LJ} and E^{tors} are the non bonded and torsional potentials respectively.

E^{LJ} uses the Lennard-Jones (LJ) potential to describe the non bonded intermolecular interactions. The LJ potential was chosen due to its wide spread use and its relative mathematical simplicity (small number of parameters) [13]. The LJ potential is given below:

$$V_{ij}^{LJ}(r_{ij}) = 4\varepsilon_{ij}\left[\left(\frac{\sigma_{ij}}{r_{ij}}\right)^{12} - \left(\frac{\sigma_{ij}}{r_{ij}}\right)^{6}\right] \tag{2.26}$$

Due to its hard repulsive wall, however, the LJ potential needs to be modified in such a way that it turns off when two molecules approach close enough, and is not repelled away by the hard repulsive wall. Also, the modification has to be done in a way so that turning the LJ potential on and off is done in a smooth manner. The modified form of E^{LJ} is given as:

$$E_{ij}^{LJ} = S(t_r)S(t_b)C_{ij}V_{ij}^{LJ}(r_{ij}) + [1 - S(t_r)]C_{ij}V_{ij}^{LJ}(r_{ij}) \qquad (2.27)$$

where $S(t)$ is a switching function while C_{ij} is a connectivity switch which ensures that there is no LJ interaction for an atom connected by a series of three or fewer bonds. t_r and t_b are given by the following expressions:

$$t_r(r_{ij}) = \frac{r_{ij} - r_{ij}^{LJ\,min}}{r_{ij}^{LJ\,max} - r_{ij}^{LJ\,min}} \qquad (2.28)$$

$$t_b(b_{ij}) = \frac{b - b_{ij}^{min}}{b_{ij}^{max} - b_{ij}^{min}} \qquad (2.29)$$

where r is the scalar distance between atoms i and j and b is the bond order. If $t < 0$, then $S(t) = 1$, while if $t > 0$, $S(t) = 0$. Applying this to E_{ij}^{LJ}, if a non-bonded atom is beyond a distance of $r_{ij}^{LJ\,max}$, then t_r is greater than zero hence $S(t_r)$ is 0. This reduces E_{ij}^{LJ} to $C_{ij}V_{ij}^{LJ}(r_{ij})$, resulting in the LJ potential to remain on. When the distance is less than

$r_{ij}^{LJ\,\max}$, then t_r is greater than zero hence $S(t_r)$ is 1, thus reducing E_{ij}^{LJ} to $S(t_b)C_{ij}V_{ij}^{LJ}(r_{ij})$.

In the case of non-bonded atoms, a hypothetical bond order is calculated with which t_b is determined. If b is less than $b_{ij}^{\max}$ $S(t_b)$ is unity hence the E_{ij}^{LJ} reduces to $C_{ij}V_{ij}^{LJ}(r_{ij})$, which indicates that a bond will not form with a non-bonded atom and said atom will instead be repelled by the hard repulsive barrier of the LJ potential. On the other hand if b is greater than $b_{ij}^{\max}$, $S(t_b)$ will be zero and therefore E_{ij}^{LJ} will be zero thus turning off the LJ potential and allowing the REBO potential to take over, since a potential bond has been formed. The REBO potential behaves in a manner identical to that described in Section 2.3.2.3.

The bond order is calculated based on the following expression:

$$b_{ij} = \frac{1}{2}[p_{ij}^{\sigma\pi} + p_{ji}^{\sigma\pi}] + \pi_{ij}^{rc} + \pi_{ij}^{dh} \tag{2.30}$$

where

$$p_{ij}^{\sigma\pi} = [1 + \sum_{k \neq i,j} w_{ik}(r_{ik})g_i(\cos\theta_{jik})e^{\lambda_{jik}} + P_{ij}]^{-\frac{1}{2}} \tag{2.31}$$

In Equations 2.30 and 2.31, P_{ij}, π_{ij}^{rc} and π_{ij}^{dh} are functions of N_{ij} which is the sum of the carbon-only and hydrogen-only coordination numbers. Thus, based on the value of N_{ij}, values of P_{ij}, π_{ij}^{rc} and π_{ij}^{dh} can be determined by the tables given in Stuart's paper [15].

The function g_i and π_{ij}^{dh}, imposes penalties on the system, that is g_i provides an angle

bending penalty, while π_{ij}^{dh} provides a penalty for rotation around multiple bonds. The

AIREBO potential improves on the areas that the Tersoff potential and REBO potential

fails, that is non-bonded interactions. This allows for systems with large numbers of

molecules, such as long chained hydrocarbons, to be simulated.

2.3.2.5 ReaxFF Potential

The ReaxFF (Reactive Force Field) potential was developed by van Duin et al

[16]. The force field expression is given as follows:

$$E_{system} = E_{bond} + E_{over} + E_{under} + E_{val} + E_{pen} + E_{tors} + E_{conj} + E_{Coulomb} + E_{vdWaals} \quad (2.32)$$

The energy term E_{bond} is defined by the following expression:

$$E_{bond} = -D_e BO_{ij} \exp[p_{be,1}(1 - BO_{ij}^{p_{be,1}})] \quad (2.33)$$

where D_e and $p_{be,1}$ pertain to bond parameters associated with carbon-carbon bonds. BO_{ij}

refers to the corrected bond order and is a function of Δ_i' and BO_{ij}^i. Both these variables

are defined below:

$$\Delta_i' = \sum_{j=1}^{nbond} BO_{ij}' - Val_i \quad (2.34)$$

$$BO'_{ij} = \exp\left[p_{bo,1}\left(\frac{r_{ij}}{r_0}\right)^{p_{bo,2}}\right] + \exp\left[p_{bo,3}\left(\frac{r_{ij}^{\pi}}{r_0}\right)^{p_{bo,4}}\right] + \exp\left[p_{bo,5}\left(\frac{r_{ij}^{\pi\pi}}{r_0}\right)^{p_{bo,6}}\right] \quad (2.35)$$

In the expression for Δ'_i, Val_i refers to the valency, which in this case, is 4 since this is an all carbon system. This is done in order to make sure the coordination of each atom is accurate. In the expression for BO'_{ij}, the p parameters are all bond parameters, while r_0, r_0^{π}, and $r_0^{\pi\pi}$ bond radii values of 1.399, 1.266 and 1.236 Å respectively. Based on the values of r_{ij}, which pertains to the distance between atoms i and j, the type of bond can be determined. In the BO'_{ij} expression, the first exponential term is 1 when r_{ij} is less than 1.5 Å and negligible at distances greater than 2.5 Å. The second exponential term is 1 when interatomic distance is less than 1.2 Å and negligible when above 1.75 Å. The third exponential term is 1 when r_{ij} is below 1 Å and is negligible above 1.4 Å. Compared to the AIREBO potential, the ReaxFF potential does not determine formation or breaking of bonds through a series of switching functions. Instead, the presence of a bond (single, double, or triple bond) is indicated by a value between 0 and 1 for each respective exponential term as shown in Equation 2.35. For example, if an atom is 2.6 Å away from another, each of the exponential term in Equation 2.35 returns a negligible value which indicates BO'_{ij} is approximately 0. Hence there are no bonds in this case. However if these atoms were at a distance of 1 Å from each other, each of the exponential terms would register 1, hence BO'_{ij} would be 3 indicating a triple bond between the two atoms.

From Equation 2.32, the terms E_{over} and E_{under} are additional energy correction terms which insure that the coordination of each carbon atom does not exceed 4 and is not below 0. The term E_{val} takes into account the energies associated with bond angles, while E_{tors} represents the energies due to dihedral angles. E_{pen} imposes a penalty on the system for situations where an atom shares two double bonds, such as in the case of allenes. E_{conj} describes the energies associated with conjugated systems such as in aromatic systems. All the energies described here takes into account only bonded atoms.

$E_{Coulomb}$ incorporates the energies associated with atomic charges and is applied to all atoms in the system regardless of bonding. In this case, there are no charges associated with each atom, hence $E_{Coulomb}$ is 0. $E_{vdWaals}$ takes into account the van der Waals forces associated with all atoms in the system. It is used to described the interactions of non-bonded atoms, and maintains a similar role as that of E^{LJ} in the AIREBO potential. $E_{vdWaals}$ is defined by the following expression:

$$E_{vdWaals} = D_{ij} \left\{ \exp\left[\alpha_{ij} \left(1 - \frac{f_{13}(r_{ij})}{r_{vdW}} \right) \right] - 2\exp\left[\frac{1}{2}\alpha_{ij} \left(1 - \frac{f_{13}(r_{ij})}{r_{vdW}} \right) \right] \right\} \qquad (2.36)$$

$$f_{13}(r_{ij}) = \left[r_{ij}^{\lambda_{29}} + \left(\frac{1}{\lambda_W} \right)^{\lambda_{28}} \right]^{\frac{1}{\lambda_{28}}} \qquad (2.37)$$

The λ terms and D_{ij} in these expressions corresponds to various energy parameters stated in the paper by van Duin [16]. The f_{13} represents a shielding term which takes into account all repulsive actions. ReaxFF, like the AIREBO potential, is a long range reactive

potential. However, ReaxFF is able to simulate ionic systems by taking into account the charges of each species in the system. This allows for systems containing oxygen, nitrogen and sulfur to be simulated. The AIREBO potential however is limited to hydrocarbon systems. Also, it uses a bond angle energy term which the AIREBO potential lacks. Table 2.1 summarizes the potentials described in Section 2.3.2, including the applicable systems and overall properties.

Table 2.1 - Summary of potentials discussed in Section 2.3.2

Potential	Properties	Applicable systems
Morse	Non-Reactive	Diatomic systems
Tersoff	Short range, Reactive	Multiatomic systems, single species, Si and C systems
REBO	Short range, Reactive	Multiatomic systems, multiple species, simple hydrocarbons, diamonds
AIREBO	Long-range, Reactive	Many-body systems with multiple species, complex hydrocarbons, diamonds, graphite
ReaxFF	Long-range, Reactive	Same as AIREBO in addition to ionic systems and systems with N_2, O_2 and S.

2.3.3 Time Integration

Once the initial positions of the molecules in a system are set, time integration is necessary to update the positions of the molecules as time progresses, based on the force field applied. This is carried out based on the numerical solutions of the second order

equations of motion. Although there are numerous methods to apply time integration, this paper will focus on the Verlet algorithm, since this is the method incorporated into LAMMPS.

According Tildesley [6], the Verlet algorithm obtains the advanced positions of the molecules by the expression:

$$r(t + \delta t) = 2r(t) - r(t - \delta t) + \delta t^2 a(t) \tag{2.38}$$

where r(t) and a(t) signifies the current position and acceleration of a particular atom, and δt is the length of the time step. The acceleration term is calculated from the forces applied on a particular atom which are described by the force field. This expression has been derived from the Taylor series expansion of r($t+\delta t$) and r($t-\delta t$) both of which are functions of velocity, that is:

$$r(t + \delta t) = r(t) + \delta t \, v(t) + \frac{\delta t^2}{2} a(t) + \ldots \tag{2.39}$$

$$r(t - \delta t) = r(t) - \delta t \, v(t) + \frac{\delta t^2}{2} a(t) + \ldots \tag{2.40}$$

The summation of these two expressions results in Equation 2.38. In order to calculate velocities, which are needed to calculate kinetic energy, the same two expressions are used, where the difference is taken resulting in the following expression:

$$v(t) = \frac{r(t + \delta t) - r(t - \delta t)}{2\delta t} \qquad (2.41)$$

Due to the discretization of the second order equations of motion, Equation 2.38 has an error of δt^4 associated with it while Equation 2.41 has an error of δt^2. In order to achieve reasonable results, a suitable time step size is necessary. Starting with the initial positions, the positions of the atoms at every subsequent time step can be calculated based on the Verlet algorithm.

CHAPTER 3

THE SIMULATION

The simulations were performed on a Red Hat Linux workstation with Intel W3520 quad-core 2.66 GHz processor and 6 GB DDR3 RAM. The simulations were performed using the LAMMPS package which was developed at Sandia National Laboratory. The package is for classical simulations only and comes built in with the reactive potentials AIREBO and ReaxFF. The AIREBO potential is usable by default when compiling LAMMPS. However, in order to run simulations with the ReaxFF potential, the *reax* package must be added before compilation. Also the Intel Fortran Compiler must be preinstalled in order for compilation with the *reax* package to be successful. The Fortran compiler is needed since the ReaxFF potential itself was written in Fortran, yet the entire LAMMPS package is written in C++.

In order to fully take advantage of the quad-core processors, parallelization is needed. MPI was installed into the workstation, allowing for LAMMPS simulations to be carried out using the four processors simultaneously. When using the AIREBO potential for a given system, half a million time steps took about 10 hours to complete. On the other hand when using the ReaxFF potential for the same system, about 10 hours was needed to complete 100000 time steps. The speed at which the AIREBO potential performs gives it an advantage over the ReaxFF potential, especially when simulating larger systems.

Simulations are performed by creating input files and in many cases data files. These files contain important commands to initiate a simulation as well as generate different output types. The input files are read line by line, from left to right, and is used to setup up the simulation box, implement the desired potential and incorporate the type of simulation, that is, NVE, NVT, and so on. Examples of input and data files are given in Appendix A. Based on the example of the input file, the commands used are explained below [17]:

1) units – This allows the user to define the type of units to be used, which also influences the values displayed in the output. Unit types relevant to this simulation are *metal* and *real*. The AIREBO potential requires the *metal* unit type, while the ReaxFF potential requires the *real* unit type. Both unit types measures distance in Angstroms; however pressure, energy and time are measured in atmospheres, kcal/mol and femtoseconds respectively for the *real* unit type, while for the *metal* unit type the respective units are bars, electron volts, and picoseconds.

2) boundary – This defines the type of boundary conditions to be used in the simulation. By default periodic boundary conditions (defined by *p*) are used; but fixed boundary conditions (defined by *f*) may also be used. The boundary conditions need to be set for each coordinate axis.

3) atom_style – This defines the type of atoms used in a simulation and the types of attributes relevant to the simulation at hand. The AIREBO potential requires the *molecular* atom style, since angle, dihedral and bond properties

must be made available for the simulation. The ReaxFF potential requires the *charge* atom style since the charges in the system are relevant to the potential.

4) read_restart/read_data − Both these commands are needed to start a simulation (assuming initial configurations are user defined). The *read_data* command requires a data file which contains information necessary for the startup of a simulation. The *read_restart* command reads a restart file (which has been created using the *write_restart* command), which is a file containing information about the state of the system at the end of a previous simulation. Using the restart file, it is possible to resume the simulation from the end point of the previous simulation.

5) pair_style/pair_coeff − The *pair_style* command allows the user to define the type of potential to be used in the simulation. To use the AIREBO potential, the command would be *pair_style airebo*. Apart from this additional information is required, that is the cutoff factor, which is a multiple of σ (equivalent to 3.4 Å for carbon-carbon interactions), and torsional and LJ flags. The torsional and LJ flags are kept as 1 to take into account torsional and LJ energies. The ReaxFF potential requires no additional input and is applied by the command *pair_style reax*. The *pair_coeff* command requires information pertinent to the potential information at hand such as parameter values. However, in the case of both the ReaxFF potential and AIREBO potential, the *pair_coeff* command is

used to link their respective input files (*ffield* and *CH.airebo* respectively) and includes the types of atoms in the system. In this case the type of atom is carbon, denoted by C for the AIREBO potential and by 1 for the ReaxFF potential.

6) fix – The *fix* command allows for the implementation of the type of simulation to be performed. In this research only two types have been implemented: (i) NVE and (ii) NPT. NVE does not require any additional parameters; however for equilibration, *fix temp/rescale* is necessary. When performing temperature rescaling, there are a number of input variables which are required. Temperature rescaling was set to be done at every time step with a desired temperature of 298 K, and the velocities were rescaled exactly so that they corresponded to the desired temperature. The *fix npt* command requires the initial and final temperature and pressure values, along with temperature and pressure damping coefficients. These damping coefficients determined the speed in which the system relaxes to the desired final temperature and pressure. Apart from the type of simulation, the *fix* command allows for time averaging throughout the simulation and a range of other functions, most of which are not relevant to this research.

7) compute – In order to analyze the simulation at hand this command is used to calculate various properties in the system which are not measured by default. This was especially helpful when calculating molecular pressures and time averaging the energies of the system. Many of the results produced

by the *compute* command can be displayed by using the *thermo_style* command.

8) thermo_style/thermo – The *thermo_style* command signifies which attributes of the system to display as outputs, such as temperature, pressure, potential energy and so on. The *thermo* command is needed to specify the time step interval for which system outputs (defined by the *thermo_style* command) are displayed. These outputs are specifically displayed in the log file.

9) dump – This command is used to generate output files. In this research, two types of output files where generated at every N number of time steps: (a) dump files, containing atom positions and stress tensors, and (b) *cfg* files, which are needed for Atomeye - a program designed for generating multiple image files of the simulation box at a given time step.

10) timestep/run – The *timestep* command designates the size of a time step while the *run* command defines the number of timesteps to perform.

The list of commands given above is the most commonly used ones in this research. Other minor commands have been used and their details can be found in the LAMMPS manual. The data file requires different pieces of information. Firstly, the system information is needed. This includes the number of atoms and atom types, the number of bonds and bond types, the number of dihedrals and dihedral types, and simulation box dimensions. In this research the bonds and dihedrals were not explicitly

stated in the data file since they were calculated by LAMMPS over the course of the simulation. The second section in the data file contains parameter information pertinent to the types of bonds, dihedrals and atoms that are used. In this case however, only atom information was given that is there was only one type of atom with a mass of 12 g/mol. The last section involves the positions of each atom in the system. These are defined in column form and includes information such as atom identification (each atom is given a numerical 'name'), atom type, molecule type (to define which atoms are part of which molecules), the Cartesian coordinates of each atoms in the box space, and, in the case of the RexaFF potential, the charge associated with each atom. With these three sections the data file, in conjunction with the input file will be able to run a stable simulation.

CHAPTER 4

RESULTS AND DISCUSSION

The first step in creating nanodiamond simulations is to produce nanodiamonds. According to Mattson et al [2], the nanodiamond molecule is created by relaxing the spherical cutout of the bulk diamond structure. They used an NVT ensemble in their quantum mechanical simulations in order to relax said bulk diamond structure.

4.1 NVE Simulations

In this research, the bulk diamond structure used consisted of 2052 carbon atoms, with interatomic spacing of 1.54 Angstroms. The bulk diamond structure resembles a spherical cutout. The bulk diamond configuration can be seen in Figure 4.1. It is clear from Figure 4.1 that the bulk diamond is nothing more than a spherical cut out from a larger diamond slab. Due to this, many carbon atoms on the surface of the bulk diamond structure are bonded to only a single carbon atom, making sites containing these atoms ideal for surface evolution into fullerene. Since both AIREBO and ReaxFF will be used for these runs, the bulk diamond relaxation must be carried out with the two potentials to determine which potential will be ideal for further simulations. Although the AIREBO potential performs faster, the ReaxFF potential should provide more accurate results. Starting with the initial bulk diamond configurations, NVE runs with temperature rescaling was conducted.
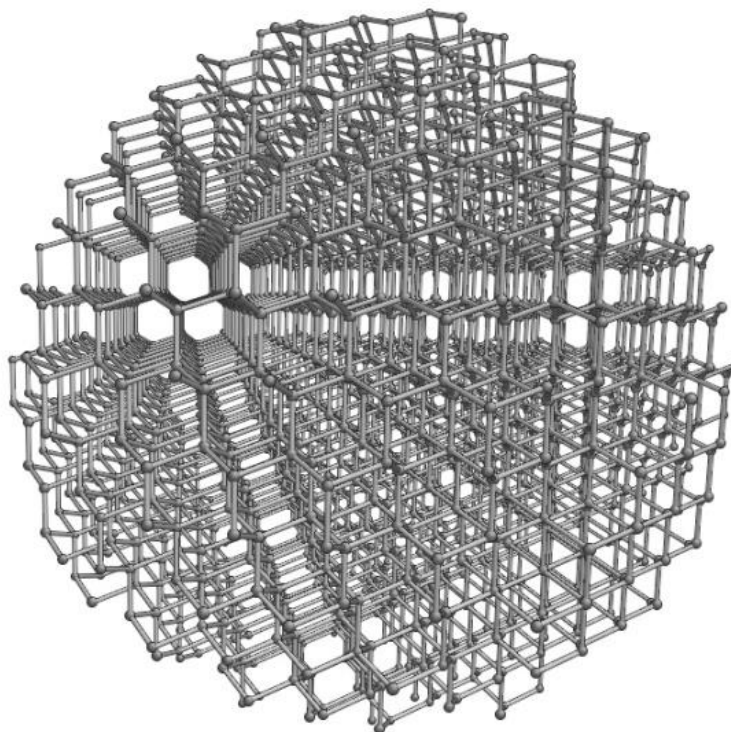
Figure 4.1 - Initial configuration of bulk diamond consisting of 2052 carbon atoms

Both NVT and NVE with temperature rescaling can be used for relaxing the structure. NVT works by adding or removing kinetic energy, as if the system was in a bath, in order to equilibrate the system at a particular temperature. NVE with temperature rescaling equilibrates the systems quite simply by scaling the velocities based on how high or low the temperature of the system is compared to the desired temperature.

The runs were completed for 1 million time steps at 0.5 fs per time step. Figure 4.2 and Figure 4.3 gives the configuration of the molecule at the end of the millionth time step. In order to further visualize the relaxation of the surface atoms into a fullerene like structure, a short Matlab code was written that would calculate the possible bond lengths

between each atom in the molecule. These bond lengths were divided into two groups: 1)

bonds which were less than 1.46 Å and 2) bonds between 1.46 and 1.7 Å. The first group

represented bond length which closely resembled fullerene bond lengths (1.42 Å), while

the latter group represented the diamond bond lengths. The orange bonds (found in most

of the figures in this paper) represent the above mentioned first group, while grey bonds
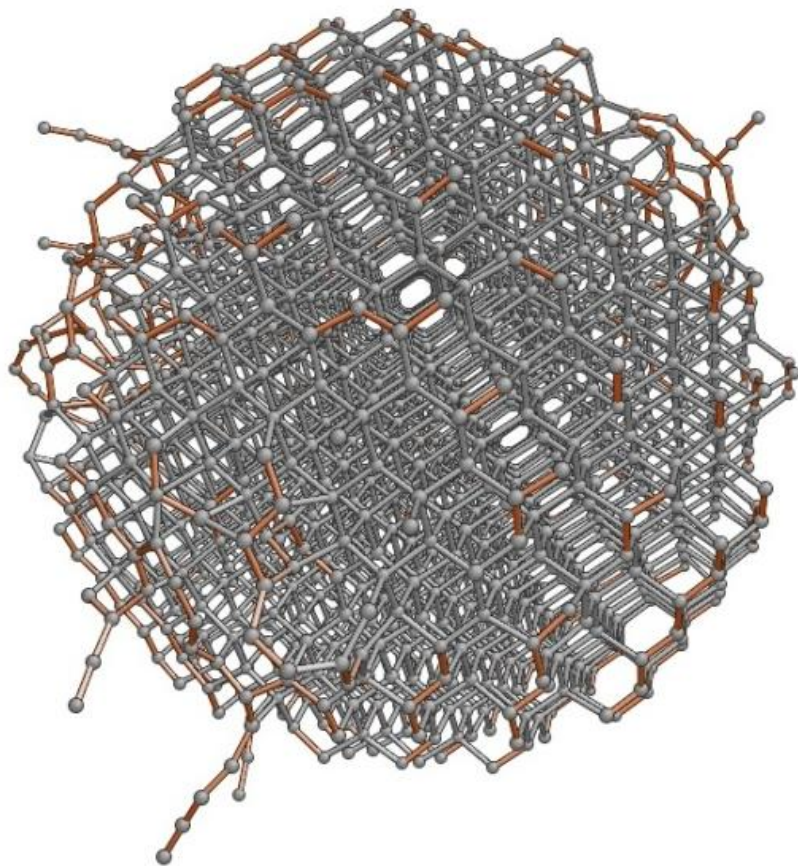
represent the latter.

**Figure 4.2 - Evolved bulk diamond structure for runs using 0.5 fs time step using the
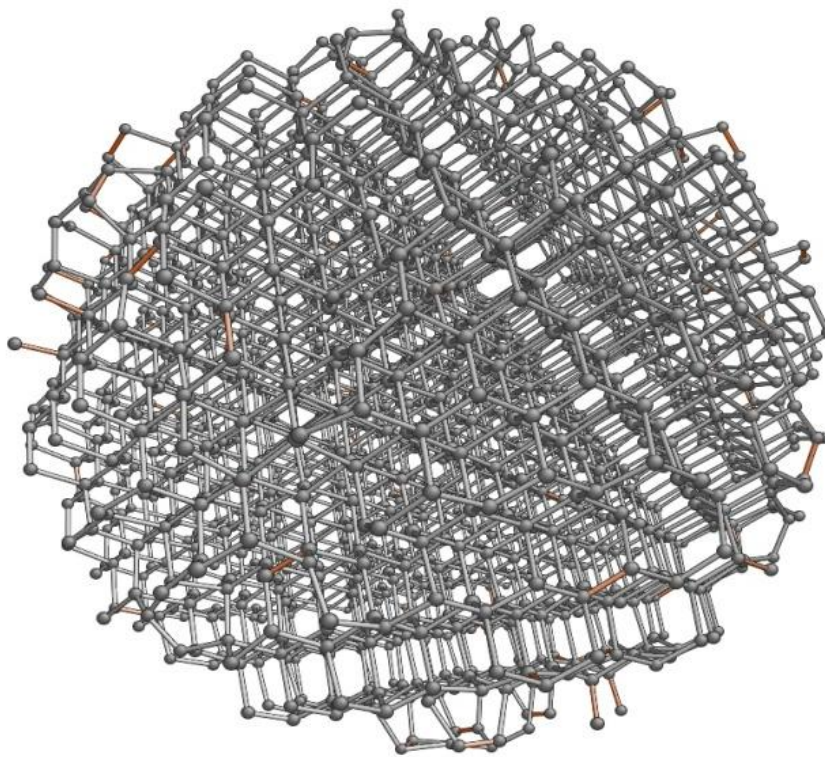AIREBO potential**

Figure 4.3 - Evolved bulk diamond structure for runs using 0.5 fs time step using the ReaxFF potential

From Figure 4.2 and Figure 4.3, it can be seen that the orange bonds representing the fullerene like bond lengths, form exclusively on the surface of the bulk diamond structure. However, there are a few differences in the manner in which the initial bulk diamond structure evolves under the two potentials. When using the AIREBO potential, a few of the atoms break away from the main diamond core while significant numbers of the surface atoms rearrange to form bonds in what seems like a haphazard mess, although there are some indications of hexagonal fullerene structure being formed. Also a large number of fullerene-like bonds can be seen on the surface. In the case of ReaxFF

potential, after one million time steps, the bulk diamond structure has evolved very little, with fullerene-like bonds few and far between. These variations in the final results give some insight into the inherent differences between the two potentials.

To ensure the previous runs produced stable structures, NVE runs (without temperature rescaling) were conducted. In both cases, the temperatures did not remain stable: the average temperatures steadily increased away from the desired temperature of 298 K. Also, the energies, contrary to the rules of an NVE run which constrains energy, did not remain constant. This clearly indicates that both structures were not fully relaxed.

Based on papers by Nielson and van Duin [18] and by Weismiller and van Duin [19], it was found that ReaxFF gave good results when using time steps of 0.1 to 0.25 fs. Since 0.5 fs was used to relax the bulk diamond structure, the larger time step contributed to the instability of the molecules. Hence, the previous run completed with the ReaxFF potential up to a million time steps at 0.5 fs, was continued using 0.1 fs and equilibrated for another million time steps. Subsequently, an NVE run was performed on the system at 0.1 fs for 100,000 time steps.

The simulation using AIREBO at 0.5 fs was continued for another million time steps at 0.1 fs was needed to relax the system. Subsequently, an NVE run was performed for 100,000 time steps. Figure 4.4 shows the bulk diamond structures of both runs after equilibration. Also, Table 4.1 shows thermodynamic properties of the system for both runs. Another simulation is currently being done using 0.1 fs starting from the initial bulk diamond configuration shown in Figure 4.1.
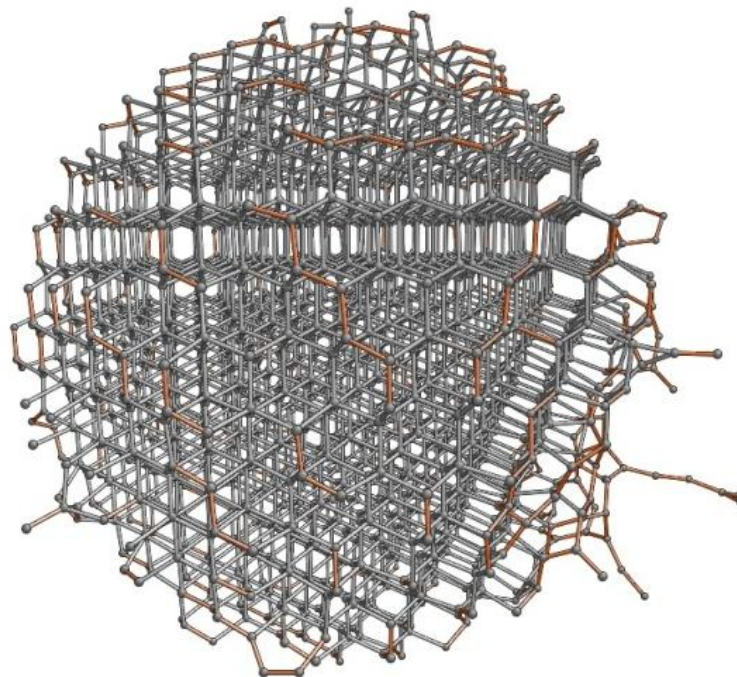
a)
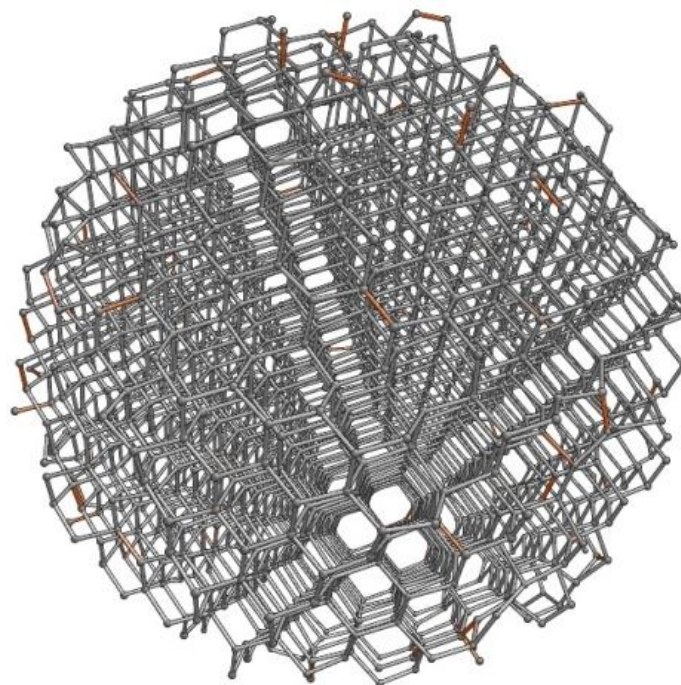
b)

Figure 4.4 - The relaxed bulk diamond structures for runs using the a) AIREBO potential and b) ReaxFF potential

Table 4.1 - Results of NVE runs of bulk diamond with ReaxFF and AIREBO potential

Potential Type	Temperature (K)	Pressure (kPa)	Potential Energy (MJ/mol)	Kinetic Energy (MJ/mol)
ReaxFF	299.694	-144.05	-1685.3	7.666
AIREBO	297.38	9.587	-1362.585	7.607

The simulations displayed the evolution of the bulk diamond in the same manner as seen in Figure 4.2 and Figure 4.3, which was done using a timestep of 0.5 fs. However, the main difference between the two sets of runs was that the later runs (with timestep of 0.1 fs) indicated stability within the molecule. Stability of the molecule was determined by the fact that the average temperature and average total energy of the system was constant. Neither run showed the evolution of the bulk diamond into the nanodiamond to the extent shown by Mattson [2].

Due to the fact that the bulk diamond structure did not fully relax into the nanodiamond structure, a hybrid structure was created by superimposing a fullerene molecule onto the bulk diamond structure. The fullerene structure in question consists of 720 carbon molecules and has an average radius of 12.59 Å. Since the radius of the bulk diamond structure is about 13 Å, some of the surface atoms of the bulk diamond structure would have to be removed, in order to ensure a stable molecule with no overlap between atoms. A Matlab code was written in order to remove atoms from the bulk diamond based on the desired radius. A suitable radius was found to be around 11.25 Å, which consisted of 1022 carbon atoms. Figure 4.5 shows the initial structure of the diamond core-fullerene hybrid.
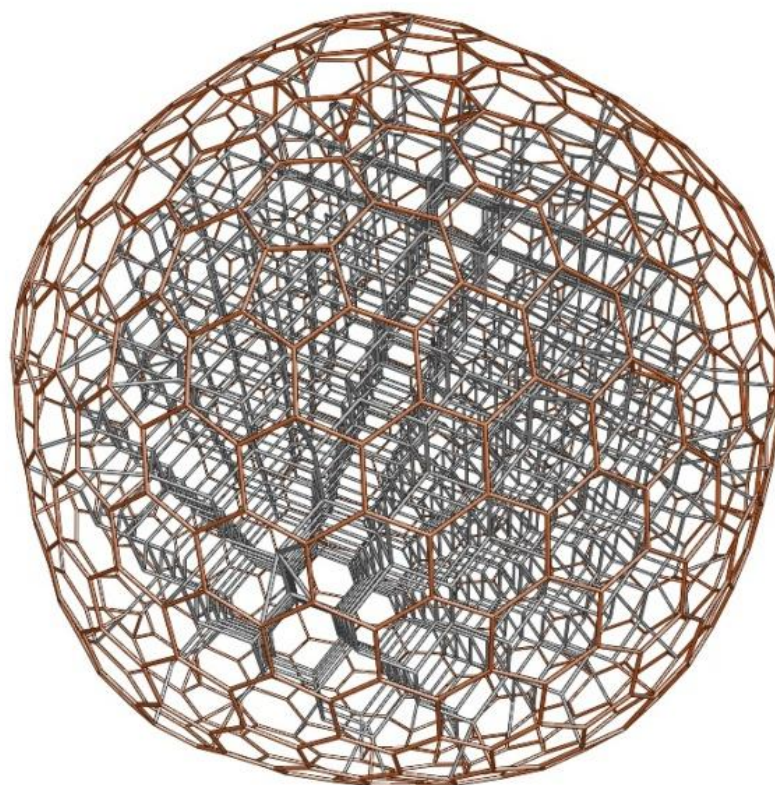
Figure 4.5 - Initial structure of 720 fullerene with 1022 carbon atom diamond core

This molecule was initially run with the ReaxFF potential at 0.5 fs for 200,000 time steps. The subsequent NVE run indicated that the molecule had not stabilized, since the temperature and energies wandered from the desired values. Of course, this was rectified when a time step of 0.1 fs was used. The equilibration runs at 0.1 fs were carried out in two ways. The first one considered the ReaxFF potential and was continued from the point where the 0.5 fs run had ended. It was carried out for 300,000 time steps. The second one involved the AIREBO potential using 0.1 fs time steps. This one was

continued from where the last run (with 0.1 fs time step for 300,000 time steps) had ended. It was carried out for 500,000 time steps. NVE runs for the set of systems were carried out at 0.1 fs for 100,000 time steps each.

The results for the runs are given in Table 4.2 and Figure 4.6. Based on the results for the equilibration runs, both molecules displayed stable temperatures and total energies. This indicates that both of these systems equilibrated. One aspect that was focused on between the two runs is the amount each molecule expands or contract from its initial configuration. The average radius of the molecule with the initial starting configuration (Figure 4.6) was 12.25 Å. The simulation which used the ReaxFF potential showed an increase in the average radius to 13.079 Å. This can also be seen in Figure 4.6a which displays a significant number of diamond-like bonds (grey-colored bonds) on the fullerene surface. This clearly indicates expansion of the molecule as the simulation progressed. In the simulation which incorporated the AIREBO potential, the average radius of the molecule reduced to 12.86 Å. This clearly indicates contraction in the molecule as the simulation progressed. The reason for this expansion and contraction rests in the differences between the mathematical expressions used for AIREBO and ReaxFF. It indicates that the attractive potential (found in E_{bond} in both expressions) is stronger for the AIREBO potential than the ReaxFF potential for the given system. Both these potentials are based on experimental results. However, researchers have shown that the ReaxFF potential is better behaved (with regards to hydrocarbon systems) compared to the AIREBO potential. This needs to be further investigated in order to confirm which potential would provide the most accurate results.

43
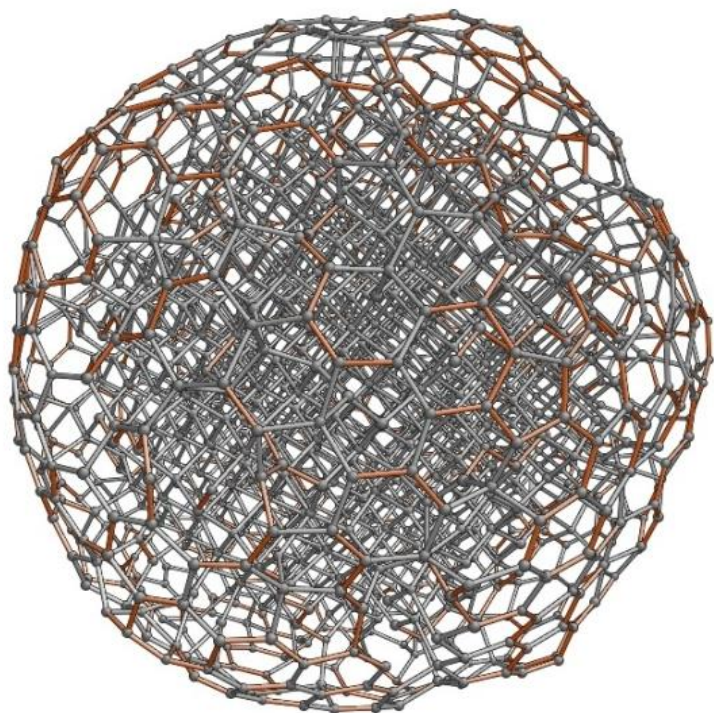
a)
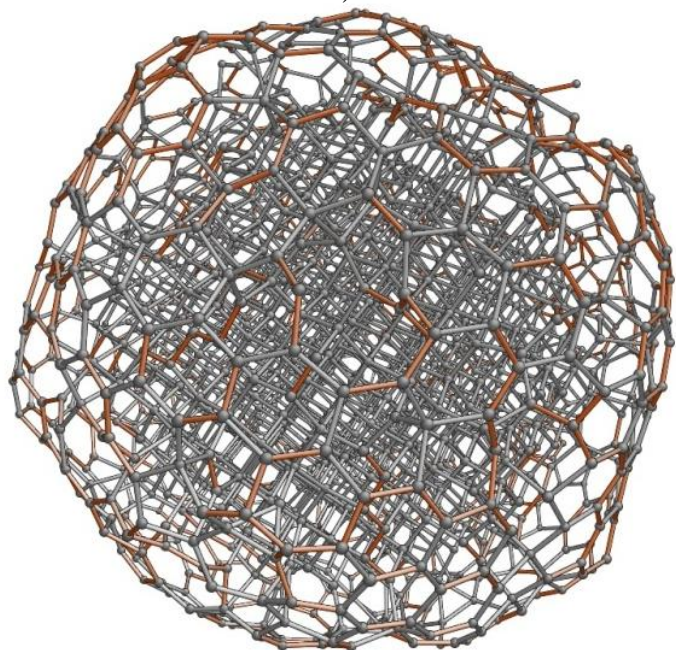
b)

Figure 4.6 - Equilibrated 720 fullerene with 1022 atom diamond core created using a) ReaxFF potential and b) AIREBO potential

Table 4.2 - Values obtained from NVE simulation of the fullerene-diamond core hybrid

Potential Type	Temperature (K)	Pressure (kPa)	Potential Energy (MJ/mol)	Kinetic Energy (MJ/mol)
ReaxFF	296.908	-6.0577	-1449.21	6.447
AIREBO	297.041	82.56	-1173.52	6.45

Another point of interest is the difference between the potential energy in runs using the AIREBO potential and runs using the ReaxFF potential. In AIREBO, the valence angles are used as a form of bond order correction in situations when two bonds are too close to each other. However, in the case of the ReaxFF potential, there is an additional term for the energy contribution of valance angles. This energy contribution needs to be studied further to confirm the reason for the difference in the energies.

4.2 NPT Simulations

Although the bulk diamond structure shows signs of evolution on the surface when performing temperature rescaling, one aspect which none of the molecules (both equilibrated and non-equilibrated) have shown is a high internal pressure. In fact the scenarios described above show very low pressures, which does not conform to the observations exhibited by Mattson [2]. In Mattson's paper, the diamond like core exhibited an internal pressure of approximately 50 GPa. In order to carry out the simulations in a more accurate manner, a pressure constraint must be imposed on the system. The pressure constraint will be applied by an NPT type of simulation.

An NPT simulation constrains both temperature and pressure. This allows for the volume and energy to fluctuate, unlike in an NVE simulation. Thermostatting is done by adding and removing kinetic energy from the system in order to maintain the desired temperature. This is done in a manner similar to an NVT simulation. Barostatting is performed by exerting the desired pressure on the simulation box. This results in the change in volume of the box so that the contents of the box experience the applied pressure. The NPT simulation is analogous to an open flask placed in ambient temperature and pressure.

The NPT simulations were carried out on the original bulk diamond structure using the AIREBO potential since said potential has the advantage of speed compared to the ReaxFF potential. The simulation was carried out in steps, that is, the desired pressure was ramped up every 50,000 time steps. These were done in steps due to the fact that relaxing the system to the desired pressure too quickly resulted in the simulation crashing. The simulation was performed for a total of 1.02 million time steps with a time step size of 0.1 fs. Eventually a system pressure of 190,000-200,000 bars was reached. Figure 4.7 shows the bulk diamond structure after undergoing the NPT simulation, while Table 4.3 shows the pressure profile of the molecule. The pressure profiles were obtained from the sum of the pressure tensors of all atoms present within a certain space divided by three times the volume of said space. The tensors (P_{xx}, P_{yy}, and P_{zz}) were calculated by LAMMPS for each atom at every thousand time steps. The dump file contained the tensors for each atom. The profiles were created using a Matlab code which read the tensors from the dump file.
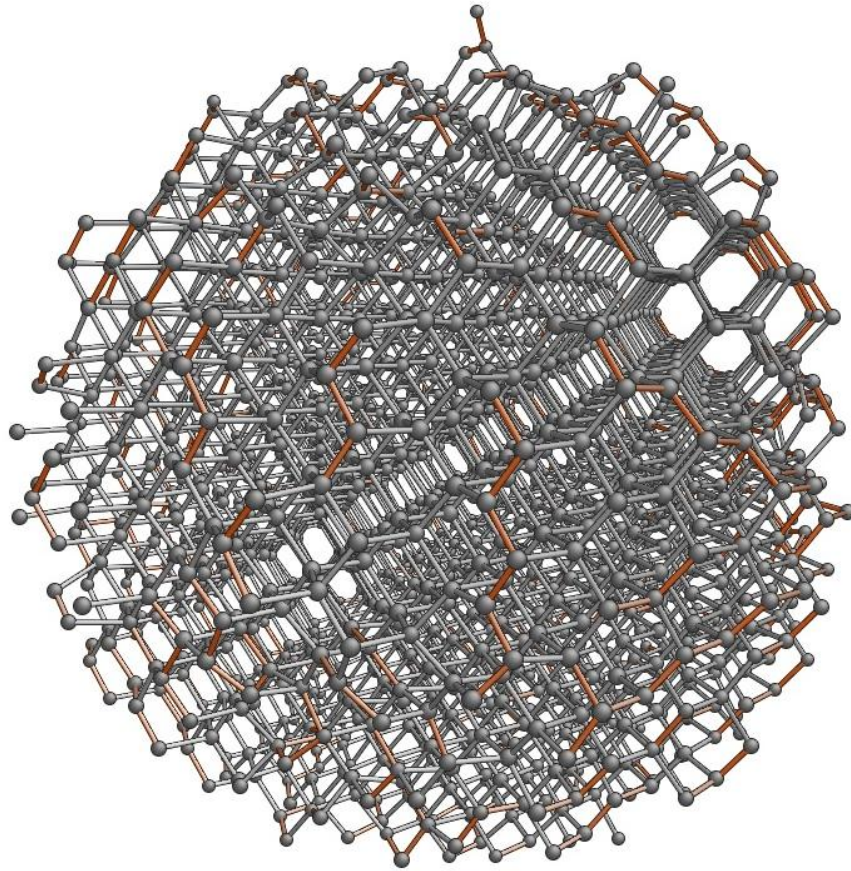
Figure 4.7 - Snapshot of the bulk diamond structure after the completion of the NPT simulation

Table 4.3 - Pressure profile of the bulk diamond after the completion of the NPT simulation

Distance from center (Angstroms)	Atoms Occupying Space	Pressure (bars)
Less than 4	62	146385
Between 4 and 8	319	150621
Between 8 and 10	365	233180
Between 10 and 11	258	303224
Between 11 and 12	363	399995
Greater than 12	685	1378965
Overall	2052	382357

In Figure 4.7, it can clearly be seen that many of the surface bonds of the bulk diamond structure are conforming to fullerene-like bonds (depicted as orange bonds). However, after an analysis of the bond lengths, it was found that approximately 10% of the bonds were fullerene-like. Also, the bulk diamond almost entirely consisted of the tetrahedral lattice structure. Table 4.3 shows the pressure profile at each layer of the molecule, including the number of carbon atoms present in each layer. Based on Table 4.3, the pressure profile indicates that the core of the bulk diamond has a pressure of about 15 GPa (volume of space with a radius of 4 Å), and the pressure increases as one moves further from the center of the molecule. This suggests that LAMMPS constrains the pressure from the outside, as opposed to each atom being subjected to the same pressure. This is evident especially in the case of the outer most layer of atoms, which experiences the largest pressures and comprises of the largest set of carbon atoms. Due to this the overall pressure of the molecule is raised to about 38 GPa.

These observations seemed to indicate that the surface was evolving slowly. In order to circumvent this, a 720 atom fullerene shell was placed over the compressed bulk diamond in a manner similar to one described previously. All atoms in the bulk diamond which are at a distance greater than 12.59 Å from the center of mass was removed (since the radius of the fullerene shell is 12.59 Å). The overlap between atoms in the fullerene shell and the surface of the bulk diamond was maintained at 1.68 Å. 948 of the 2052 atoms from the bulk diamond core was used in the simulation. Due to the fact that an unpressurized fullerene shell was placed over highly pressurized diamond core, some care was taken when initiating the simulation. The time step size was reduced to as low

as 0.005 fs, while the pressure constraint was reduced to 50,000 bars initially. The pressure and time step size was increased every 10,000-20,000 time steps. A total of 1.5 million time steps were performed in order to equilibrate the system out of which 1 million time steps were done using a step size of 0.1 fs. The maximum system pressure achieved using this configuration was 140,000 bars. A Figure 4.8 shows the nanodiamond after 1.5 million time steps. Table 4.4 displays the pressure profile of the molecule.
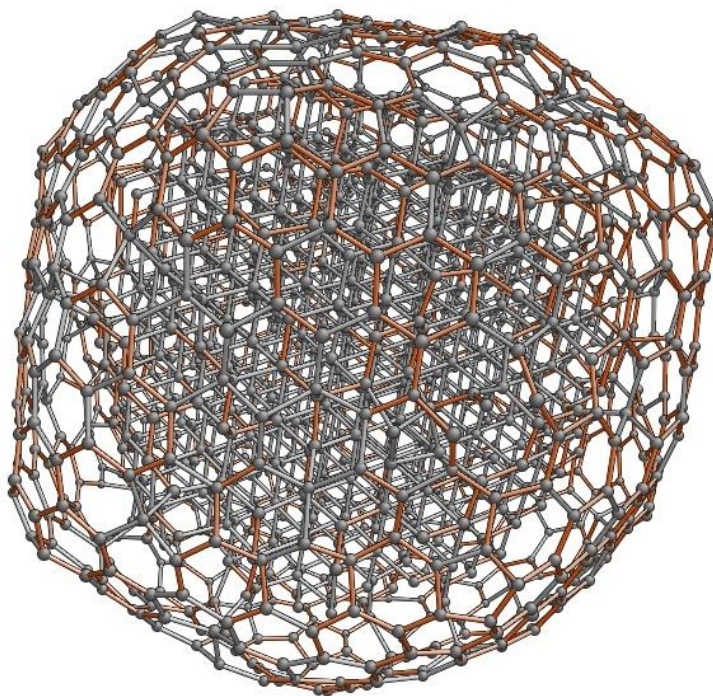

Figure 4.8 - Nanodiamond after 1.5 million time steps

Table 4.4 - Pressure profile of the nanodiamond after 1.5 million time steps

Distance from center (Angstroms)	Atoms Occupying Space	Pressure (bars)
Less than 4	60	507479
Between 4 and 8	357	409087
Between 8 and 10	402	590911
Between 10 and 11	130	250998
Between 11 and 12	173	124072
Greater than 12	546	303049
Overall	1668	306702

From Table 4.4, it can be seen that the core has been pressurized to about 50 GPa. At a distance of 10-12 Å from the center, a drop in pressure can be seen. This is due to the void space present between the fullerene shell and the diamond core. This is an indication that the fullerene shell is compressing the diamond core further than seen in Table 4.3. To insure that this structure (including the internal pressure) will hold, an NVE run is performed for 400,000 time steps, after 1.5 million time steps of temperature rescaling. The results of the NVE run are given in Table 4.5. The pressure profiles are given in Table 4.6. Comparing the pressure profile before and after the pressure constraint is removed, it is clear to see that the core pressures drop during the NVE simulations. In fact the drop in pressure is about 60%. The overall pressure of the molecule was also reduced significantly, although this is due to the fact that the outermost layer of atoms (greater than 12 Å) contributed very low pressures to the overall. The low pressures exhibited by the outer most atoms are due to the fact that they are in contact with empty space. The pressure indicated by Table 4.5 indicates the overall pressure for the entire simulation box. Since most of the box consists of void space, a low

overall pressure was expected. Such a large pressure drop can be attributed to the fact that a large overlap was taken (1.68 Å) and the core was allowed to relax once the pressure constraint was removed. In order to confirm this, another nanodiamond is created using a smaller overlap (1.62 Å).

Table 4.5 – NVE results after 400,000 time steps

Potential Type	Temperature (K)	Pressure (kPa)	Potential Energy (MJ/mol)	Kinetic Energy (MJ/mol)
AIREBO	300.849	-52.497	-1166.88	6.48

Table 4.6 - Pressure profile of the nanodiamond after the completion of the NVE runs

Distance from center (Angstroms)	Atoms Occupying Space	Pressure (bars)
Less than 4	56	174560
Between 4 and 8	336	147429
Between 8 and 10	390	273320
Between 10 and 11	158	228300
Between 11 and 12	57	-28070
Greater than 12	671	-81162
Overall	1668	801.215

This second nanodiamond was created with an overlap of 1.62 Å. This molecule contains 976 atoms in the diamond core, with a 720 carbon atom fullerene shell. The method used to create this molecule is identical to that used in the previous case (overlap 1.68 Å). The pressure constraint was set at 150,000 bars, and a time step size of 0.0005 fs

was used to initiate the simulation. The size of the time step was slowly increased until 0.1 fs was reached. A total of 155,000 time steps were used when the pressure was constrained. Figure 4.9 shows the structure of this nanodiamond, while Table 4.7 provides the pressure profile of said molecule. By comparing the Figure 4.9 and Figure 4.8, it can be seen that the overall structure of both the molecules look the same, that is the makeup of fullerene like bonds are concentrated on the surface of the molecule and about 30% of all the bonds are fullerene like, which is what was observed with the previous nanodiamond. Table 4.7 shows that this nanodiamond has a slightly higher internal pressure. In fact, it is about 2 GPa higher than that observed in the previous case.
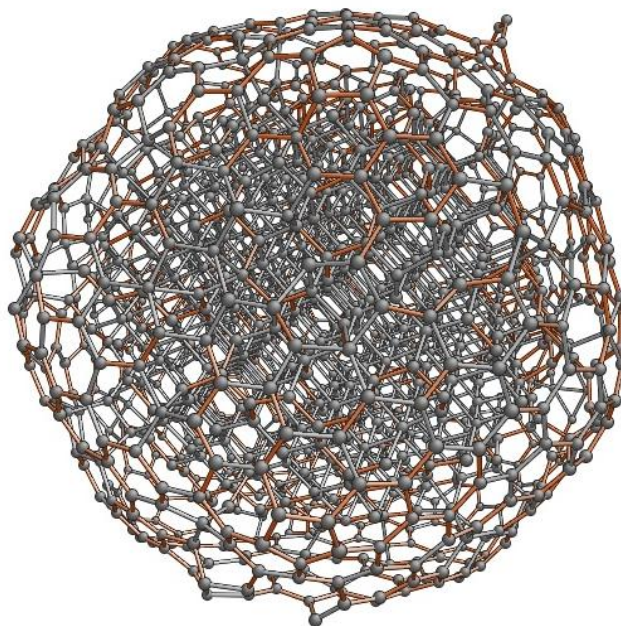

Figure 4.9 - Nanodiamond with overlap of 1.62 Å

Table 4.7 - Pressure profile of the nanodiamond with overlap of 1.62 Å prior to NVE run

Distance from center (Angstroms)	Atoms Occupying Space	Pressure (bars)
Less than 4	65	521120
Between 4 and 8	360	469858
Between 8 and 10	403	666477
Between 10 and 11	140	251698
Between 11 and 12	179	138034
Greater than 12	549	-132719
Overall	1696	349776

The true test of the molecule is when the pressure constraint is removed. Initially temperature rescaling was done in order to equilibrate the system. This was done for 3 million time steps at 0.1 fs. The NVE run was performed for 100,000 time steps, and the pressure profiles and average measurements for the system for said run are given in Tables 4.8 and 4.9 respectively. Based on Table 4.8, it can be seen that there is a pressure drop (also exhibited by the previous molecule), however the core of this molecule retains a higher pressure than the previous molecule. This can be attributed by the fact that there are more atoms in the same volume than in the previous case. A large portion of carbon atoms can be found at a distance greater than 12 Å from the center and since their pressures are very low, the overall pressure of the molecule is reduced. The pressure in Table 4.9 indicates the overall pressure of the simulation box. Since the box is mostly void space a low average pressure was expected. Low pressures were also expected in the region between the fullerene shell and the diamond core (the overlap) due to the presence of void space.

Table 4.8 - Pressure profile of the nanodiamond with overlap of 1.62 Å after NVE run

Distance from center (Angstroms)	Atoms Occupying Space	Pressure (bars)
Less than 4	65	201373
Between 4 and 8	314	138592
Between 8 and 10	396	249335
Between 10 and 11	186	232844
Between 11 and 12	56	-11642.9
Greater than 12	679	-49457
Overall	1696	-92.759

Table 4.9 – NVE results for nanodiamond with overlap of 1.62 Å

Potential Type	Temperature (K)	Pressure (kPa)	Potential Energy (MJ/mol)	Kinetic Energy (MJ/mol)
AIREBO	296.92	10.8413	-1183.7	6.505

Some of the structural properties of both the nanodiamonds described above are given in Table 4.10. As one can see, about 30% of the bonds in each molecule are fullerene-like. The second molecule has more diamond bonds than the first, since it contains more atoms in the diamond core. The average bond lengths for the diamond core in each molecule are shorter than the bulk diamond bond length of 1.54 Å. This clearly shows that the cores are compressed. This compression was observed by Mattson et al [2], and is the main factor contributing to SBE in the nanodiamond. Investigations must be carried out to determine if the diamond core can be further compressed. Even a reduction of 0.01 Å of average bond length will translate to a greater SBE.

Table 4.10 – Structural properties of both nanodiamonds

Nanodiamond Overlap (Å)	No. of Fullerene bonds	No. of Diamond bonds	Fullerene bond length (Å)	Diamond bond length (Å)	% Fullerene bonds
1.68	971	1860	1.417±0.031	1.513±0.037	34.29
1.62	970	1929	1.415±0.032	1.516±0.041	33.46

4.3 General Process of Creating Nanodiamonds

These simulations have created two types of stable nanodiamonds, as described by Mattson et al [2]. In creating these two molecules, the same process was applied. This process can also be used to create more nanodiamonds with varying degrees of overlap. The overall process is given below in a step wise manner.

1) Starting with the bulk diamond structure, an NPT simulation was performed with a pressure constraint of 200,000 bars. This was done to compress the bulk diamond structure, and as shown in Table 4.3, the pressure is seen to increase from the inside of the bulk diamond to the outside.

2) With the compressed diamond core, it is necessary to reduce the radius by removing surface atoms from the bulk diamond. This was done so that it would fit into the fullerene shell (radius of 12.59 Å). This was done in a two step process. The first step involves removing all atoms from the bulk diamond which are greater than 12.59 Å from the center. This is done with a Matlab code. A second Matlab code is used for the second process, which involves removing atoms from the bulk diamond based on their distance from the fullerene shell. This determines the size of the overlap. This

overlap is crucial, since a smaller overlap would mean too many fullerene atoms are close to the bulk diamond, which would rupture the fullerene shell. A ruptured shell will not be able to hold the core pressure and allow it to relax, which is not wanted. Once an overlap size has been set, the fullerene is placed over the diamond core.

3) A data file is created which contains the initial positions of the desired diamond core/fullerene shell. An NPT simulation is started with the desired pressure of 150,000-200,000 bars. The step size is reduced to a point where the simulation will seize to crash.

4) Starting at the smallest possible step size, the simulation is performed in steps, that is 5,000-20,000 time steps are completed every time the step size is increased.

5) Once the desired pressure has been reached, the NVE runs are started. In order to make sure the core pressure is sufficient, a Matlab code was used to find the pressure based on the pressure tensors reported by the LAMMPS output. The positions of the atoms in the molecule at the end of the NPT simulation are used to create another data file. The size of the simulation box should be at least 3 Å greater than the diameter of the nanodiamond. The boundary settings are switched from period to fixed for these simulations.

6)   Temperature rescaling is performed until the system equilibrates, after which an NVE run is done. Pressure profiles are obtained as desired using the Matlab code described previously.

This approach will be needed to produce nanodiamonds with a smaller overlap. However, a method must be developed in order to alter the structure of the fullerene shell (by removing certain carbon atoms). By altering the shell, more pentagonal structure are formed as opposed to hexagonal structures which will tighten the shell around the diamond core. All this is necessary in order to preserve the core pressure of the nanodiamond when the pressure constraint is removed.

CHAPTER 5

CONCLUSION AND RECOMMENDATIONS

The simulations used in this research allowed for the creation of a stable nanodiamond. These nanodiamonds were made based on the observed reports provided by Mattson et al [2]. They also retained a large portion of their core pressure even after the pressure constraint was removed. However, the nanodiamond cores still experience a pressure loss of about 60% when the pressure constraint is removed. A systematic approach in creating stable nanodiamonds was developed and is applicable for the creation of different types of nanodiamonds. These stable nanodiamonds can be used for further research into SBE.

Two areas can be researched further based on the above mentioned stable nanodiamonds:

1) Although a nanodiamond was created with an overlap of 1.62 Å, the minimum overlap allowed can be determined by creating a series of nanodiamonds with smaller overlaps.

2) The stable nanodiamonds can be used for high velocity collisions between each other in order to determine the rate of SBER. Since molecular dynamic simulations use a fraction of the computing power used by quantum simulations it will be possible to perform these collisions using multiple

nanodiamonds. The size of the system is dependent on the computing power of the current workstation.

The minimum overlap needs to be found in order for the nanodiamond to retain most of its core pressure when the pressure constraint is removed. Also in regards to preserving the core pressure, it is also necessary to develop a method through which the fullerene surface structure can be modified in order to provide a tighter fit around the diamond core. This would require removing key carbon atoms, in the fullerene shell, in such a way that the shell forms (when equilibrated) more pentagonal structures as opposed to hexagonal structures. Also, this has to be done while making sure the minimum overlap is maintained. Once these steps are carried out, the nanodiamond will be able to maintain its core pressure to satisfactory amount, and the collision simulations carried out using this molecule will provide accurate results.

REFERENCES

[1]   Raty, J.Y.; Galli, G.; 'Optical properties and structures of nanodiamonds', *Journal of Electroanalytical Chemistry*, vol. 584, no. 1. pp 9-12, October 2005

[2]   Mattson, W.D.; Balu, R.; Rice, B.M.; Ciezak, J.A.; 'Exploiting unique features of nanodiamonds as an advanced energy source', *ARL-TR-4783*, April 2009

[3]   Titov, V.M.; Tolochko, B.P.; Ten, K.A.; Lukyanchikov, L.A.; Pruuel, E.R.; 'Where and when are nanodiamonds formed under explosion?', *Diamond and Related Materials*, vol. 16, no. 12. pp 2009-2013, September 2007

[4]   Brodka, A.; Hawelek, L.; Burian, A.; Tomita, S.; Honkimaki, V.; 'Molecular dynamics study of structure and graphitization process of nanodiamonds', *Journal of Molecular Structure*, vol. 887, no. 1-3, pp. 34-40, January 2008

[5]   Barnard, A.S.; Sternberg, M.; 'Substitutional nitrogen in nanodiamond and bucky-diamond particles', *Journal of Physical Chemistry*, vol. 109, no. 36, pp. 17107-17112, July 2005

[6]   Tildesley, D.J.; Allen, M.P.; *Computer simulations of liquids*, Clarendon Press, 2003

[7]   Melchionna, S.; Ciccotti, G.; Holian, B.L.; 'Hoover NPT dynamics for systems varying in shape and size', *Molecular Physics*, vol. 78, no. 3, pp. 533-544, July 1993

[8]   Goldstein, H.; Poole, C.; Safko, J.; *Classical Mechanics*, 3rd edition, Addison-Wesley, 2002

[9]   Evans, D.J.; 'On the representation of orientation space', *Molecular Physics*, vol. 34, no. 2, pp. 317-325, 1977

[10]   Pauling, L.; 'Atomic radii and interatomic distances in metals', *Journal of American Chemical Society*, vol. 69, no. 3, pp. 542-553, March 1947

[11]   Brenner, D.W.; 'Empirical potential for hydrocarbons for use in simulating the chemical vapor deposition of diamond films', *Physical Review B*, vol. 42, no. 15, pp. 9458-9471, July 1990

[12]   Morse, P.M.; 'Diatomic molecules according to the wave mechanics. II. Vibrational levels', *Physical Review*, vol. 34, no. 1, pp. 57-64, July 1929

[13]   Tersoff, J.; 'New empirical approach for the structure and energy of covalent systems', *Physical Review B*, vol. 37, no. 12, pp. 6991-7000, August 1987

[14]   Brenner, D.W.; Shenderova, O.A.; Harrison, J.A.; Stuart, S.J.; Ni, B.; Sinnott, S.B.; 'A second generation reactive empirical bond order (REBO) potential energy expression for hydrocarbons', *Journal of Physics: Condensed Matter*, vol. 14, no. 4, pp. 783-802, January 2002

[15]   Stuart, S.J.; Tutein, A.B.; Harrison, J.A.; 'A reactive potential for hydrocarbons with intermolecular interactions', *Journal of Chemical Physics*, vol. 112, no. 14, pp. 6472-6486, January 2000

[16]   van Duin, A.C.T.; Dasgupta, S.; Lorant, F.; Goddard, W.A.; 'ReaxFF: A reactive force field for hydrocarbons', *Journal of Physical Chemistry*, vol. 105, no. 105, pp. 9396-9409, March 2001

[17]   Sandia National Laboratory; 'LAMMPS user's manual', http://lammps.sandia.gov, Sandia Corporation, 2003

[18]   Nielson, K.; van Duin, A.; Oxgaard, J.; Deng, W.; Goddard, W.; 'Development of the ReaxFF Reactive Force Field for Describing Transition Metal Catalyzed Reaction, with Application to the Initial Stages of the Catalytic Formation of Carbon Nanotubes', *Journal of Physical Chemistry A*, vol. 109, no. 3, pp. 493-499, January 2005

[19]   Weismiller, M.; van Duin, A.; Lee, J.; Yetter, R.; 'ReaxFF Reactive Force Field Development and Application for Molecular Dynamics Simulations of Ammonia Borane Dehydrogenation and Combustion', *Journal of. Physical Chemistry A*, vol. 114, no. 17, pp. 5485-5492, April 2010

APPENDIX

EXAMPLES OF INPUT SCRIPTS AND DATA FILES FOR LAMMPS

Given below is an example of an input script used to perform simulations on LAMMPS. The simulation to be performed based on the example calls for a 50,000 time step run starting from a restart file *bulknptfull20.nano*. *Metal* units are being used which uses picoseconds for time, Angstroms for length, Kelvin for temperature, bars for pressure, and eV for energy. The force field is set to the AIREBO potential with a cutoff factor of 3.5 for an all carbon system. An NVE run is to be done with temperature rescaling to a desired temperature of 298 K. Pressure tensors will be calculated and written into the *dump* file. Apart from the *dump* file, *cfg* files will also be created every 1,000 time steps. A restart start file will be created and a time step size of 0.0001 picoseconds will be set.

```
units metal
atom_style molecular
dimension 3


read_restart bulknptfull20.nano
pair_style airebo 3.5 1 1
pair_coeff * * CH.airebo C

fix 2 all temp/rescale 1 298 298 0.1 1
fix 1 all nve

compute press all stress/atom
compute 2 all reduce sum c_press[1] c_press[2] c_press[3]
variable p equal -(c_2[1]+c_2[2]+c_2[3])/(3*8359)

timestep 0.0001
log log.npt21
neigh_modify one 2800 page 500000
thermo_style custom step temp press etotal pe epair v_p
thermo 100
dump 1 all custom 1000 nptnew.dump id mol x y z c_press[1] c_press[2]
c_press[3]
dump 2 all cfg 1000 ndnew.*.cfg id type xs ys zs
dump_modify 2 element C
run 50000
write_restart bulknptfull21.nano
```

Given below is an example of a data file. The simulation box size is set to a length of 33 in the x,y, and z direction. The system contains 1890 atoms of 1 atom type. The mass of the single atom type (named 1) is 12 g/mole. The x, y, and z coordinates of each atom is given. Apart from the coordinates, an id number is attached to each atom. The columns of 1 pertain to the atom type number and the molecule id.

```
LAMMPS Description

1890 atoms
1 atom types

0 33 xlo xhi
0 33 ylo yhi
0 33 zlo zhi

Masses

1 12.0

Atoms

1     1     1     14.571195339600    6.483250726800    6.948817725600
2     1     1     15.785967882000    6.434616711000    7.483465277400
3     1     1     13.752778594200    7.565512723800    7.174611514200
4     1     1     12.269000172600    7.802542309200    7.917839875200
5     1     1     21.446980386000    6.331012212600    4.621211367000
6     1     1     21.383354420400    7.632600882600    4.726971570600
7     1     1     6.428998812600    13.364588347200   7.632960166800
8     1     1     6.634901321400    12.009988926600   7.537782516000
9     1     1     7.493525235000    14.563062451800   7.777523064000
10    1     1     7.123299198000    10.803675894000   7.902913249800
11    1     1     5.987993788200    14.908857163200   7.634527952400
12    1     1     9.227169486600    10.957482193800   4.981410108600
13    1     1     10.000087787400   10.908390907200   6.186286004400
14    1     1     11.478313635000   10.908162271800   5.913425985600
```